Prestrain relaxation in non-covalently modified ethylene-vinyl acetate | PyChol | multiwall carbon nanotube nanocomposites

Campo, E.; Winter, A.D.; Jaye, C.; Fischer, D.; Omastova, M.; Campo, E.M.

APL Materials

DOI:
10.1063/1.4884216

Published: 23/06/2014

Publisher's PDF, also known as Version of record

Prestrain relaxation in non-covalently modified ethylene-vinyl acetate | PyChol | multiwall carbon nanotube nanocomposites

A. D. Winter, C. Jaye, D. Fischer, M. Omastová, and E. M. Campo

Citation: APL Materials **2**, 066105 (2014); doi: 10.1063/1.4884216
View online: http://dx.doi.org/10.1063/1.4884216
View Table of Contents: http://scitation.aip.org/content/aip/journal/aplmater/2/6?ver=pdfcov
Published by the AIP Publishing

APL MATERIALS **2**, 066105 (2014)

Prestrain relaxation in non-covalently modified ethylene-vinyl acetate | PyChol | multiwall carbon nanotube nanocomposites

A. D. Winter,[1] C. Jaye,[2] D. Fischer,[2] M. Omastová,[3] and E. M. Campo[1,a]
[1]*School of Electronic Engineering, Bangor University, Bangor UK LL57 1UT, United Kingdom*
[2]*Material Measurement Laboratory, National Institute of Standards and Technology, Gaithersburg, Maryland 20899, USA*
[3]*Polymer Institute, Slovak Academy of Sciences, Bratislava SK 84541, Slovakia*

(Received 13 March 2014; accepted 8 June 2014; published online 23 June 2014)

Effects of aging on chemical structure and molecular dynamic behaviour of strained thermally active ethylene-vinyl acetate | multiwall carbon nanotube (EVA|MWCNT) composites were investigated by spectroscopy and microscopy techniques. Aged composites showed spatial inhomogeneity due to system relaxation. Inhomogeneity is attributed to segregation of non-covalently linked cholestryl 1-pyrenecarboxylate, acting as MWCNT dispersant and polymer compatibilizer. Analysis of molecular interplay between filler and matrix upon *in situ* temperature variation showed a lack of synchronicity, which had been observed in fresh composites. Reduced synchronous interplay allowed quantification of degraded π-π interactions, promoting PyChol unlatching as a result of both sonication and strained-derived π-π degradation. [http://dx.doi.org/10.1063/1.4884216]

Recently, a variety of polymer systems have exhibited mechanical response upon external stimuli.[1] In this scheme, thermal, optical, or electrical stimulus triggers a reversible change in dimension, that can be tailored to promote folding/unfolding in smart packaging,[2] raise/lower a microstructure for tactile perception,[3] and promote the contraction of an artificial muscle.[4] Albeit, the possibility of scaling the system from the nanometer to the macro-scale, as well as response to multiple stimuli, reversible character, and potential low cost are all attractive properties of smart nanocomposites in a range of fields, from Micro-Opto-Electro-Mechanical Systems (MOEMS) and nanotechnology to neuroscience and tissue engineering.[5,6] Multiwall carbon nanotube (MWCNT) polymer composites are amongst the material systems prone to thermal actuation.[3] However, a major challenge in the fabrication of nanocomposites is achieving a homogeneous dispersion of nanotubes, since van der Waal forces promote nanotube bundling, interrupting a still-to-be-elucidated electronic dialog between fillers and matrix.[7] Although sonication and shear mixing are common dispersing procedures, they often result in nanotube fracture and surface damage.[8] Another approach towards filler dispersion is the addition of surfactants or dispersants, either through covalent or non-covalent interactions.[9] Photoactuation has recently been observed in ethylene-vinyl acetate | multiwall carbon nanotubes (EVA|MWCNT) composites, where dispersion of MWCNT was achieved by non-covalently bonding cholestryl 1-pyrenecarboxylate (PyChol) to pristine MWCNT walls.[3] In this scenario, the actuation mechanism was modelled as light being absorbed by MWCNTs and quickly being converted to local heat. Heat would then be transferred to surrounding polymeric chains, which would relax and contract, resulting in macroscopic mechanical actuation. Further, applied prestrain

[a]Author to whom correspondence should be addressed. Electronic mail: e.campo@bangor.ac.uk.

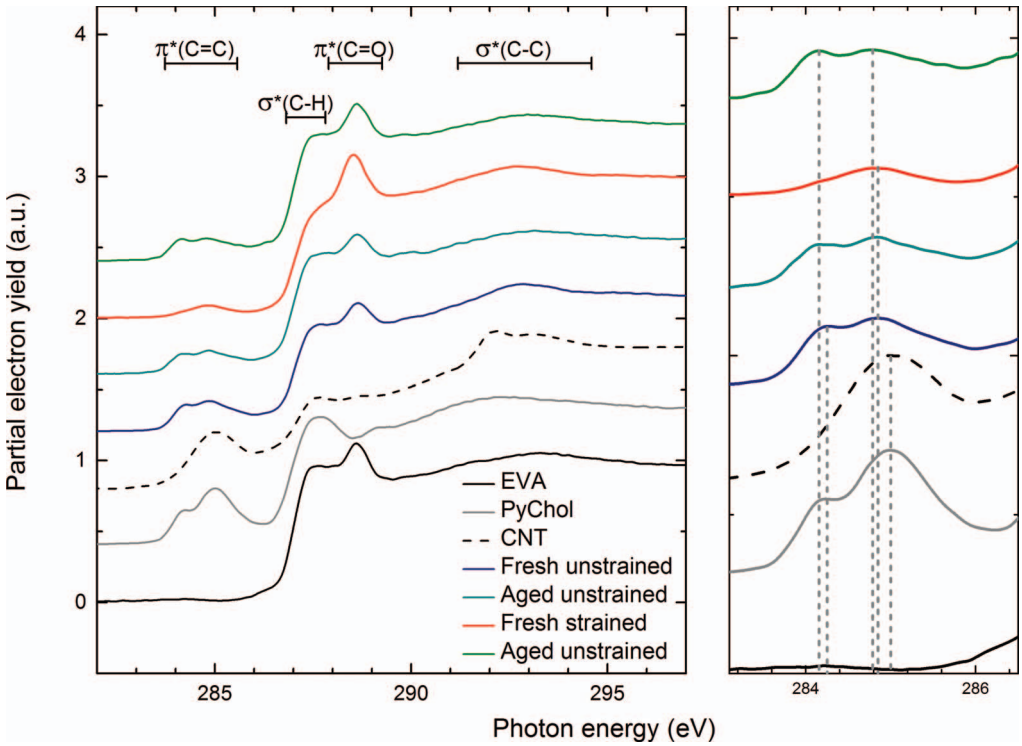

FIG. 1. NEXAFS spectra of aged unstrained and prestrained composites at room temperature (left). Interplays of energies and intensities of π^* C=C resonances (right).

is a critical aspect in mechanically responsive systems, the extent of which determines expansive or contractile output behavior.[10,11] The mechanisms behind this phenomenon remain unknown. The atomistic phenomena in systems displaying both modes of actuation have been proposed to be identical; exclusively resulting from a contractile response of individual nanotubes due to kinks further deforming upon excitation. The average response of the system would then be contractive or expansive, uniquely as a function of the extent of filler alignment.

We have recently reported temperature resolved *in situ* Near Edge X-Ray Absorption Fine Structure (NEXAFS) on thermo-active EVA|MWCNT composites, in an effort to correlate macroscopic actuation to spectral variations.[12] By probing unoccupied states, NEXAFS spectroscopy offers invaluable information about a system's chemical environment and structural composition.[13] Temperature-variable NEXAFS spectra had revealed synchronous interplay between π^* C=C and π^* C=O resonances, suggesting conformational variations between polymer chains and MWCNTs as a result of latching through CH-π interactions. Spectral variations with temperature were more pronounced in prestrained versus unstrained composites, which is consistent with findings at the macroscopic level, where strained systems correlated with enhanced mechanical response upon thermal stimulus.[14] We are now interested in studying the molecular durability of these composites as a vehicle to explore the molecular communication between MWCNT, PyChol, and EVA as they relate to fabrication (involving mixing, sonication, and straining) and further relaxation upon aging. In this work, we address effects of aging by conducting *in situ* temperature-resolved NEXAFS spectroscopy and Atomic Force Microscopy (AFM) imaging on identically processed composites as those reported earlier.[12] Description of experimental procedures can be found in the supplementary material.[15]

Figure 1 shows room temperature C K-edge NEXAFS spectra of EVA, PyChol, MWCNT, fresh (shortly after manufacturing), and aged (a year after manufacturing) composites, which have either been subjected to prestrain or not. EVA spectrum shows three resonances at 287.0 eV, 288.6 eV, and 293.0 eV attributed to $1s \rightarrow \sigma^*_{C-H}$, $1s \rightarrow \pi^*_{C=O}$, and $1s \rightarrow \sigma^*_{C-C}$ transitions, respectively.

TABLE I. Energy and intensity values of π^*_1 C=C, π^*_2 C=C, and π^* C=O NEXAFS resonances.

System	C=C π^*_2[a] (eV)	ΔC=C π^*_2[b] (eV)	π^*_1 intensity (a.u.)	π^*_2 intensity (a.u.)	C=O π^* (eV)	ΔC=O π^*[c] (eV)	C=O π^* intensity (a.u.)
PyChol	285.0	...	0.25	0.40	...	...	...
Pristine EVA	...	...	...	...	288.6	...	1.13
Fresh unstrained	284.9	−0.1	0.18	0.22	288.6	0	0.91
Fresh prestrained	284.9	−0.1	0.06	0.09	288.5	−0.1	1.17
Aged unstrained	284.8	−0.2	0.15	0.17	288.6	0	1.00
Aged prestrained	284.8	−0.2	0.16	0.16	288.6	0	1.06

[a]π^*_2 C=C refers to resonance of phenyl groups in PyChol and MWCNT walls.
[b]$\Delta\pi^*_2$ C=C is calculated against the reference provided by PyChol.
[c]$\Delta\pi^*$ C=O is calculated against the reference provided by EVA.

The same resonances observed in EVA appear in PyChol, albeit with different intensities. PyChol spectrum presents additional resonances at 284.2 eV and 285.0 eV, both corresponding to 1s → $\pi^*_{C=C}$ transitions. We attribute π^*_1 (284.2 eV) and π^*_2 (285.0 eV) C=C to cholesteryl and pyrene groups, respectively, the latter assigned per the graphitic structure of pyrene[16] (Figure S1 of the supplementary material).[15] MWCNTs also show 1s → $\pi^*_{C=C}$ resonances at 285.0 eV, as well as 1s → σ^*_{C-C} transitions around 293 eV. Resonances within the energy range 287–290 eV indicate the presence of oxygenated states on the MWCNT lattice.[17]

Spectral signatures from EVA and PyChol standards are summarised in Table I. NEXAFS spectra of composites (fresh unstrained composite, Figure 1) appear similar to that of pristine EVA at high energies. Resonances at low energies reflect the addition of fillers and dispersant. The 1s → π^*_2 C=C resonance, contributed to by MWCNTs and PyChol, appears downshifted by 0.1 eV (Table I). This resonance has been found at 285.0 eV in both MWCNTs and PyChol. The shifted resonance highlights new molecular interactions in the composites.[13] We tentatively attribute this shift to π-π interactions, as established between MWCNTs and PyChol, during high frequency sonication.[3] This proposal, however, is in disagreement with Kocharova *et al.*,[18] who correlated π-π interactions in Single wall carbon nanotubes (SWCNTs) with an energy upshift in π^*_2 C=C resonances. Albeit, π-π interactions are likely bonding mechanisms between MWCNT and PyChol, and good MWCNT dispersion and PyChol coverage was observed upon fabrication.[3]

Further, π^*_1 C=C showed no shift upon mixing, suggesting cholesteryl groups are not involved in MWCNT-PyChol interactions (Figure 2(a)). Indeed, the desired purpose of cholesteryl groups was to prevent MWCNT bundling by acting as "spacers."[3] The interplay of intensities in the fresh unstrained composite is strongly influenced by the matrix, where π^*_1 and π^*_2 C=C signals are attenuated (with respect to the standards) since these states are now less available to the incident beam. Further, the relative intensity of both resonances ($\pi^*_1 : \pi^*_2 = 0.61$ in PyChol) is also modified ($\pi^*_1 : \pi^*_2 = 0.81$ in fresh unstrained) owing to conformational effects of π^*_2 versus the high degree of freedom in π^*_1 from the cholesteryl group. Figure 2 shows orbital (above) and molecular (center) interactions, as well as conformation relations (below) between MWCNTs, PyChol, and EVA. Panels (a), (b), and (c) correlate with mixing/sonication, straining, and aging, respectively. During mixing (Figure 2(a)), π-π interactions are established between MWCNTs and PyChol, and EVA appends to PyChol through CH-π interactions.

No further energy shift is observed in the π^*_2 C=C system upon straining (fresh strained composite, Figure 1). A downshift of 0.1 eV (Table I) is observed on the π^* C=O resonance, possibly indicating modification on the chemical environment at the vicinity of C=O groups resulting from straining. Decreased π^*_2 C=C resonances and increased π^* C=O has also been attributed to strain-induced MWCNT alignment and highlights the interconnectivity of π^* C=O from EVA and π^*_2 C=C from the PyChol-CNT ensemble (Figure 2(b)).[12] In fact, we have reported improved thermal response from (fresh) prestrained composites, which we tentatively attribute to improved interfacial connectivity, i.e., stronger π-π interactions that have been facilitated upon straining (Figure 2(b)).

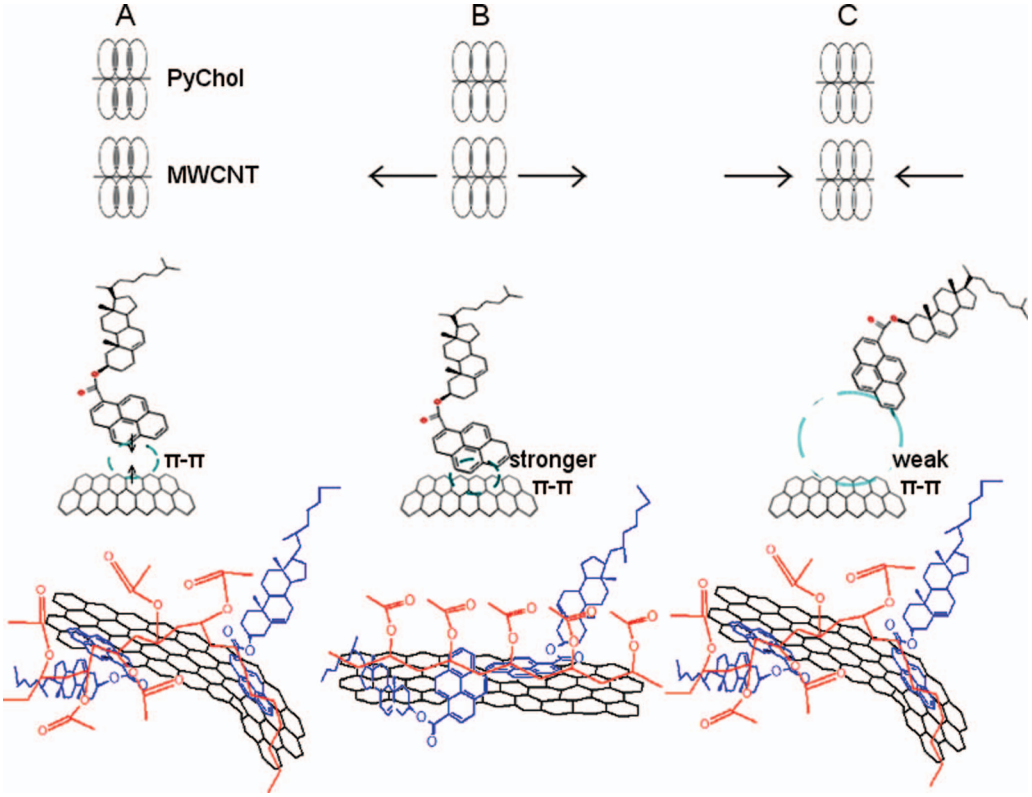

FIG. 2. Proposed model of interactions of EVA|PyChol|MWCNT composites. EVA Polymer (red) shown as only vinyl acetate for simplicity. (a) PyChol molecules (blue) are latched to MWCNTs (black) through π-π interactions formed during sonication; and EVA bond through CH-π interactions resulting in isotropic C=O groups. (b) Through applied prestrain MWCNTs align along plane and C=O groups from EVA exist in isotropic configuration. (c) On aging π-π interactions between PyChol and MWCNTs are no longer viable, which leads to PyChol unlatching and terminating communication between EVA and MWCNT. Predicted evoluion of π-π dynamics are highlighted in the three stages.

We propose the externally provided elastic energy could be stored in a modified metastable π-π system. This point will be addressed further throughout this discussion.

Upon aging, an upshift of 0.1 eV is observed in π^* C=O, back to the unstrained stage (aged prestrained, Table I). Local chemical sensitivity in NEXAFS,[13] suggests the neighbouring atoms to C=O are relaxing back to the original state prior to straining. Further, π^*_2 C=C and π^* C=O intensities increase and decrease, respectively, reversing the conformational trends originally seen upon straining, also pointing at relaxation.[12] A possible mechanism conducive to non-conforming EVA chains is through PyChol unlatching. In this scheme, π-π interactions are no longer viable and connectivity between MWCNTs and EVA is lost (Figure 2(c)). In fact, the stored energy in the proposed metastable bonding state in Figure 2(b) could, upon release (aging), act as the driving force towards increased entropy in a PyChol-segregating scheme.

To address the possibility of PyChol segregation in aged prestrained composites, we acquired NEXAFS spectra and AFM maps in different locations. Differences in spectra acquired at room temperature on three different locations (Figure S4 of the supplementary material)[15] suggest a degradation of spatial homogeneity. The largest intensity variation is observed for σ^* C–C and π^*_1 C=C resonances, both attributed to PyChol. This is significantly more evident for the prestrained composite and would support increased PyChol segregation augmented with input strain. Topographic and phase AFM characterisation of aged prestrained composites at two scales (scanned regions 50 μm and 15 μm above and below, respectively) are shown in Figure S5 of the supplementary material.[15] Elongated structures in topographic mode (Figures S5(a) and S5(c) of the

supplementary material)[15] are associated with MWCNTs, and the matrix shows some roughness in the background.

Phase imaging (Figures S5(b) and S5(d) of the supplementary material)[15] is sensitive to mechanical properties, such as Young's modulus (E), viscoelasticity, and adhesion. Although incapable of quantitative determination of E, phase contrast suffices to differentiate systems whose mechanical responses yield segregated soft and hard phases.[19] It has been previously established that in soft and moderate tapping modes (for values 20% and above of driving to set point amplitude) a stiffer phase would yield increased phase variation, showing as bright contrast in AFM phase images.[20] Also, adhesion and damping arguments predict less dissipation in crystalline phases versus increased damping and dissipation in amorphous systems, yielding bright and dark phase contrast, respectively.[19] By correlating topography and phase imaging, two distinct phases can be easily identified in Figures S5(b) and S5(d) of the supplementary material;[15] EVA matrix (dark background phase) and PyChol (bright phase). Indeed, Huang and co-workers found E_{EVA} 0.01 GPa[21] and although E_{PyChol} has not been reported, as-synthesized PyChol shows a clear crystalline character, versus amorphous EVA. This analysis further supports the notion that PyChol is segregating away from the MWCNTs into the EVA matrix upon aging, since bright regions around MWCNTs (Figure S5(d) of the supplementary material)[15] correspond to deposits of unlatched PyChol at the MWCNT surface, as depicted in Figure 2(c). Our earlier prediction of elastic energy being stored in modified metastable π-π systems is coherent with the increasingly entropic composite seen in AFM.

We had observed an increased conformational response from strained composites during temperature-resolved NEXAFS altogether,[12] suggesting stronger π-π interactions. Incidentally, the notion of stronger π-π interactions upon mechanical straining bears reminiscence to catch bonds in biophysics.[22] Upon conventional (slip) bonding, bond lifetimes and strengths decrease with applied tensile force.[23,24] However, catch bonds show a maximum in their lifetimes at a nonzero applied force.[25] Indeed, response of biological systems to applied forces, such as protein adhesion to Eukariotic cells,[23] is critical to understanding cell binding and resilience from pervasive environmental forces within living organisms. In this scheme, slip and catch bonds derive from a variety of potential energy landscapes, promoting strain engineering of individual bonds.[26] This could be an early report to suggest the existence of catch bonds outside the context of biophysics; tying up with previously predicted nanomechanical interlocking in polymer/CNT ensembles upon straining.[27]

Remarkably, a quantitative account of aging can be derived by examining the dynamics of NEXAFS spectra upon thermal excitation. We had reported earlier on temperature-resolved NEXAFS spectra of fresh composites.[12] These results led to the hypothesis that as the polymeric chains interact with MWCNTs through CH-π interactions, C=O groups from EVA are anisotropically distributed with respect to the tube axis. Upon irradiation, MWCNTs are excited and experience torsional strain, yielding an isotropic distribution of C=O groups. This model is consistent with previous mechanisms where MWCNTs twist and form kinks upon excitation.[14] Also consistent with macroscopic findings, we had observed the largest response from prestrained composites, for which resonance intensities showed at least 4 times greater variation with temperature than unstrained composites.[12]

In aged systems, temperature-resolved spectra shows slight increases in π^*_2 C=C in both strained and unstrained composites (Figure S6 of the supplementary material).[15] However, π^* C=O resonances vary some in unstrained and remain fairly constant in prestrained composites. This is an important finding, as it suggests lack of communication between torsional tubes and conforming polymeric chains. The physics of this missing synchronicity resonates with the proposed model in Figure 2(c), where unlatched PyChol can no longer communicate filler and matrix. Temperature-resolved NEXAFS show aging has had an impact in both strained and unstrained composites, suggesting that π-π interactions in these systems have a certain lifetime ($\tau_{\pi\text{-}\pi}$, resulting from sonication). However, unlatching has been more prevalent in the prestrained system, with minimum communication between MWCNTs and EVA. This is, again, consistent with a more entropic system, driven by released energy (Figure 2(c)) previously stored in metastable π-π systems (Figure 2(b)). Echoing previous linear analysis performed in fresh samples, Table II describes intensity trend variations (Tv, as described earlier)[12] of aged π^*_2 C=C and π^* C=O.

TABLE II. Intensity trends derived from temperature-resolved NEXAFS of aged composites.

		Ratios	
	Linear fits to NEXAFS intensities	π^*_2 C=C/π^* C=O	Strained/unstrained
π^*_2 C=C strained	$y = 0.027x - 0.80$	$T_{vC=C} = -54T_{vC=O}$	$T_{v\ C=C\ strained} = 3T_{v\ C=C\ unstrained}$
π^* C=O strained	$y = -0.0005x + 0.02$		$T_{v\ C=O\ strained} = 0.17T_{v\ C=O\ unstrained}$
π^*_2 C=C unstrained	$y = 0.012x - 0.37$	$T_{vC=C} = -4T_{vC=O}$	
π^* C=O unstrained	$y = -0.003x + 0.08$		

Reiterating the fact that variations of π^*_2 C=C and π^* C=O with temperature are correlated through PyChol bonding, alterations in the trends upon aging, are likely related to variations in PyChol bonding (Figure 2(c)). Indeed, by comparing Tv in the fresh and aged scenarios,[12] quantification of aging effects on the molecular structure can be provided. Since spectral variations are observed upon aging in both strained and unstrained composites, and consistent with the model proposed in Figure 2, we predict two aging mechanisms are promoting total π-π degradation (A_T). The first mechanism affects the lifetime of π-π sonicated-derived interactions ($A_{\pi\text{-}\pi}$) between PyChol molecules and MWCNTs, resulting from mixing and sonication. The second mechanism derives from prestrain relaxation ($A\varepsilon$):

$$A_T = A_{\pi-\pi} + A\varepsilon. \quad (1)$$

Unstrained composites will exclusively undergo sonicated-derived aging. In this scenario, most PyChol molecules provide some degree of interconnectivity between MWCNTs and EVA (π^*_2 C=C/π^* C=O synchronicity in Figure S6 of the supplementary material,[15] below), and $T_{v\ C=C}/T_{v\ C=O}$ is a measure of this interconnectivity, according to the actuation model.[12] Since aged and fresh $T_{v\ C=C}/T_{v\ C=O}$ were −4 and −5, respectively, we find 20% of PyChol molecules unlatched upon sonicated-derived aging ($A_{\pi\text{-}\pi} = 20\%$).

Notably, aged strained composites loose synchronicity (Figure S6 of the supplementary material,[15] above): variations in π^*_2 C=C do not correlate with variations in π^* C=O, in agreement with the unlatching process proposed in Figure 2. In this scenario, their ratio (−54) lacks physical meaning, since the number of PyChol molecules still attached to the MWCNTs is insufficient to confer MWCNTs and EVA adequate connectivity. An alternative method to quantify A_T in aged prestrained composites is to address how the $T_{v\ C=O\ strained}/T_{v\ C=O\ unstrained}$ ratios evolved upon aging. Indeed, by observing how temperature responses evolve in contemporary systems-strained and unstrained, the degree of connectivity can be estimated. In fresh composites $T_{v\ C=O\ strained}/T_{v\ C=O\ unstrained} = 4$ correlates with 100% PyChol coverage,[12] and the ratio (0.17) found in aged composites (Table II), therefore, correlates with only 4% PyChol coverage, and 96% has unlatched. In conclusion, we found synthetic procedures and 1 year aging in these composites yield a total aging $A_T = 96\%$, where $A_{\pi\text{-}\pi} = 20\%$ and strain-relaxation derived aging accounts for $A\varepsilon = 76\%$. The proposed model offers an indication to potential energy landscapes, similar to those involved in catch bond dynamics,[22] and strain-induced reactivity.[26] It is worth highlighting the impact of these findings, placing emphasis on the importance of processing towards the formation and evolution of π-π interactions. Further studies aim at correlating thermodynamics associated with processing conditions and resulting molecular interplay, since those will determine the durability of nanocomposites towards microsystem technology adoption.

In this work, we have identified π-π interactions in EVA|PyChol|MWCNT composites by way of a π^*_2 C=C shift in NEXAFS spectra. These π-π interactions have a limited lifetime, by comparing molecular variations from strained and unstrained composites analysed through NEXAFS shortly after synthesis, or 12 months later. Indeed, *in situ* temperature analysis no longer showed a synchronous response between π^* C=C and π^* C=O resonances in aged composites, suggesting a disordered system that was also confirmed by AFM imaging. The proposed model of a π-π bonded PyChol|MWCNT system is processing and time-dependant, with stronger π-π interaction upon straining. This description is in good agreement with nanomechanical interlocking in nanocomposites and catch bonds in biophysics. Upon aging, and as a consequence of processing, PyChol, used as

dispersant and compatibilizer, unlatches and segregates. Remarkably, both strained and unstrained systems underwent molecular disorder, indicative of both sonication and strain serving as driving forces towards PyChol segregation. Albeit, strained composites showed increased signs of PyChol segregation and molecular disorder. Intensity trends observed upon temperature variations have concluded that 96% of the original PyChol has unlatched in strained composites, where 20% is due to sonication effects and 76% is due to straining effects. These are important considerations towards microsystem manufacturing to ensure device longevity. Finally, whether a library of electronic configurations is behind, the reported bimodal responses remain to be addressed.

Research was carried out in part at the National Synchrotron Light Source at Brookhaven National Laboratory, which is supported by the U.S. Department of Energy under Contract No. DE-AC02-98CH10886. This project was partially founded by FP7 VEGA 2/0149/14 and NMP 22896. Certain commercial names are presented in this manuscript for purposes of illustration and do not constitute an endorsement by the National Institute of Standards and Technology. The authors acknowledge K. Czanikova for assistance in composite synthesis, F. A. Alamgir and C. R. Weiland for helpful discussions on the realm of synchrotron spectroscopy.

[1] L. Ionov, J. Mater. Chem. **20**, 3382 (2010).
[2] T. Ikeda and T. Ube, Mater. Today **14**, 480 (2011).
[3] K. Czaniková, I. Krupa, M. Ilčíková, P. Kasák, D. Chorvár, M. Valentin, M. Šlouf, J. Mosnáček, M. Mičušík, and M. Omastová, J. Nanophotonics 063522_1 (2011).
[4] Y. Bar-Cohen, Handbook Biomimetics **11**, 1 (2000).
[5] L. Sun, W. M. Huang, Z. Ding, Y. Zhao, C. C. Wang, H. Purnawali, and C. Tang, Mater. Des. **33**, 577 (2012).
[6] J. Loomis, B. King, T. Burkhead, P. Xu, N. Bessler, E. Terentjev, and B. Panchapakesan, Nanotechnology **23**, 045501 (2012).
[7] M. Moniruzzaman and K. I. Winey, Macromolecules **39**, 5194 (2006).
[8] Y. Y. Huang and E. M. Terentjev, Polymers **4**, 275 (2012).
[9] J. Yu, B. Tonpheng, G. Gröbner, and O. Andersson, Macromolecules **45**, 2841 (2012).
[10] R. Vaia, Nat. Mater. **4**, 429 (2005).
[11] S. V. Ahir and E. M. Terentjev, Nat. Mater. **4**, 491 (2005).
[12] A. D. Winter, E. Larios, F. A. Alamgir, C. Jaye, D. Fischer, M. Omastová, and E. M. Campo, J. Phys. Chem. C **118**, 3733 (2014).
[13] J. Stöhr, *NEXAFS Spectroscopy* (Springer, 2003).
[14] S. V. Ahir, A. M. Squires, A. R. Tajbakhsh, and E. M. Terentjev, Phys. Rev. B **73**, 085420 (2006).
[15] See supplementary material at http://dx.doi.org/10.1063/1.4884216 for detailed experimental methods (synthesis and characterization) and additional characterization NEXAFS.
[16] V. Lee, C. Park, C. Jaye, D. A. Fischer, Q. Yu, W. Wu, Z. Liu, J. Bao, S.-S. Pei, C. Smith, P. Lysaght, and S. Banerjee, J. Phys. Chem. Lett. **1**, 1247 (2010).
[17] S. Banerjee, T. Hemraj-Benny, M. Balasubramanian, D. Fischer, J. A. Misewich, and S. S. Wong, ChemPhysChem **5**, 1416 (2004).
[18] N. Kocharova, J. Leiro, J. Lukkari, M. Heinonen, T. Skála, F. Šutara, M. Skoda, and M. Vondráček, Langmuir **24**, 3235 (2008).
[19] P. Schön, K. Bagdi, K. Molnár, P. Markus, B. Pukánszky, and G. Julius Vancso, Eur. Polym. J. **47**, 692 (2011).
[20] S. N. Magonov and D. H. Reneker, Annu. Rev. Mater. Sci. **27**, 175 (1997).
[21] N. H. Huang, Z. J. Chen, C. H. Yi, and J. Q. Wang, Exp. Polym. Lett. **4**, 227 (2010).
[22] S. Rakshit and S. Sivasankar, Phys. Chem. Chem. Phys. **16**, 2211 (2014).
[23] G. Bell, Science **200**, 618 (1978).
[24] W. E. Thomas, V. Vogel, and E. Sokurenko, Annu. Rev. Biophys. **37**, 399 (2008).
[25] H. Chen and A. Alexander-Katz, Biophys. J. **100**, 174 (2011).
[26] B. Yildiz, MRS Bull. **39**, 147 (2014).
[27] M. Wong, M. Paramsothy, X. J. Xu, Y. Ren, S. Li, and K. Liao, Polymer **44**, 7757 (2003).